4.0 AERATORS ON SPILLWAYS

P Volkart* & P Rutschmann**

* Head of the Dam Hydraulic Section of the Laboratory of Hydraulics, Hydrology and Glaciology of the Federal Institute of Technology, Zurich, Switzerland.

** Senior research Engineer of the Laboratory of Hydraulics, Hydrology and Glaciology of the Federal Institute of Technology, Zurich, Switzerland.

4.1 Introduction

The past decade has witnessed an increase in the height of dams and in the specific flow rates discharged down spillways. On many projects dam heights are in excess of 200 m with spillway discharges greater than 270 m^3/m sec. These quantities imply velocities in the concrete spillway chutes of the order of 50 m/sec and higher.

As the flow velocity at the boundary of a hydraulic structure increases, the potential for damage to the structure by cavitation erosion also increases. Indeed cavitation erosion damage increases approximately with the 6th power of the velocity and once small cavities occur in a concrete surface they can reach depths of several metres within a relatively short time.

The inception of cavitation erosion depends to a large extent on the surface finish of the hydraulic structure. As velocities increase above a certain limit, the surface finish required to prevent cavitation erosion exceeds the tolerance to be expected from standard construction practice. With velocities greater than about 22 to 26 m/s protection of the flow boundary by means of streamlining, lining critical areas with steel sheets, using improved surface finishes and/or cavitation erosion resistant

materials, is neither economic nor completely successful. In these cases the spillway surface is usually protected from cavitation damage by introducing air near the spillway floor section. Devices called aerators which supply the air are located on the spillway floor. Offsets in the lateral walls are also often provided to ensure aeration all around the jet. A typical aerator is shown in Fig. 4.1.

Aerators are normally placed in the region where the natural aeration has not reached the spillway floor (Chapter 3). The flow in the aerator region is deflected from the floor by a ramp; both the lower and the upper surfaces break up into droplets, and air is entrained into the main flow. The air demand from the lower surface causes air to flow from the sides of the spillway through the side duct. The entrained air on the lower surface appears as bubbles concentrated near the spillway floor.

The following topics - important to the design engineer - are discussed in this chapter:

- The need for aerators
- The location and number of aerators
- The importance of the geometry of the aerators and the aerator supply system
- The necessity for model studies
- The effect of aerators on downstream conditions
- A suggested design procedure

A short discussion on cavitation and the manner in which air bubbles appear to prevent its occurrence is also included.

4.2 Cavitation

Cavitation occurs when the absolute pressure in the interior of the fluid falls to the vapour pressure of the fluid. At this point the tensile stresses in the interior of the fluid cause small pockets of vapour to form within the fluid. These are transported to high pressure regions where they collapse. This collapse, which occurs over a very short time, results in pressure shocks of high intensity and frequency close to the walls and

channel bottom. These cause alternating stresses on the boundary material and cavitation erosion. The formation of the vapour bubbles is almost instantaneous, and thus, although the mean pressure in the flow may be above the local vapour pressure, turbulent fluctuations or disturbances coming from any local roughnesses (such as the displacement caused by concrete joints, longitudinal ribs and poor construction) may trigger cavitation.

Some frequent causes of cavitation erosion on spillway chutes are shown schematically in Fig. 4.2(a) and (b). The most important hydraulic parameters to be considered are the flow velocity u, the local atmospheric pressure p_a, the local surface pressure p, and the amplitudes of the pressure fluctuations and the vapour pressure of the fluid p_v (a function of the local atmospheric pressure). With moderate flow velocities, it is possible to protect a channel's concrete surface by having a very smooth finish with a high degree of hardness.

The effects of the vapour bubble collapse is proportional to the mean velocity and this leads to a cavitation parameter of the form

$$\kappa = \frac{(p - p_v)}{\rho_w u^2_2} \qquad 4.1$$

On a spillway with a vertical curvature and negligible air entrainment the local pressure (p) may be computed from

$$p = p_a + \rho_w h \left(g \cos\alpha \pm \frac{u^2}{r} \right) \qquad 4.2$$

where h = flow depth normal to surface

α = angle between the bottom and horizontal

r = radius of curvature of the boundary

g = acceleration due to gravity

\+ is used for concave boundary curvature

\- is used for convex.

A decrease in the cavitation parameter κ increases the tendency to cavitation damage.

Cavitation damage to spillway boundaries, providing they have a good finish, will not occur under usual operating conditions if the cavitation parameter κ exceeds a value of approximately 0.25 (Falvey, 1984). This value implies that cavitation may occur at velocities in excess of 29 m/s for concrete spillways of good finish with no vertical curvature and not at high altitude. However, the maximum cavitation free velocity is probably lower, in the range 22-26 m/s.

Peterka in 1953 showed that small volumes of air near a concrete surface can greatly reduce cavitation damage. He performed tests on concrete in a cavitation apparatus for a period of two hours, and with velocities of up to 35 m/s. The weight loss of the concrete is plotted versus air concentration in Fig. 4.3. This figure shows that a small air bubble concentration c of about 1 to 2% reduces cavitation erosion markedly, and that with an air concentration near the bottom of the flow section of 6 to 8%, cavitation erosion virtually ceases. Russel and Sheehan (1974) performed tests for high head outlet works using 7.5 cm square closed conduit and showed that in their apparatus air concentrations of 3 to 5% were sufficient to prevent cavitation erosion for velocities up to 46 m/s. These tests are indicative only as the velocity profiles and boundary layer thickness would be different from those on a chute spillway.

Additional investigations by Galperin et al. (1981) showed that the air concentration required for protection also depends on concrete strength and flow velocity (Fig. 4.4). Further, Ball (1976) showed that the maximum allowable flow velocity which will not induce cavitation erosion depends on the size and spacing of surface irregularities. However, the influence of surface roughness nearly vanishes if the flow section is sufficiently aerated near the bottom.

The precise mechanism by which the small air concentrations protect the concrete surface is unclear, but small air concentrations decrease the velocity of a compression wave (Fig. 4.5) and hence any shock pressures.

The ratio of the number of introduced air bubbles to the boundary area, i.e. the effective bubble distribution, is important for prevention of cavitation erosion. Thus, the average air concentration near the bottom or sides of the flow section is a necessary but - theoretically - not sufficient criteria at the design stage. (An average air concentration can correspond to different bubble distributions.) If flow velocities exceed 35 m/s, the limited state of knowledge makes the use of conservative values of c advisable. Clearly, aeration systems must be designed so that they cannot become submerged and so that air can be entrained over the full width of the spillway.

4.3 The Mechanisms Affecting Air Entrainment

From the brief discussion on cavitation the object of bottom aerators is thus to introduce small air concentrations near the spillway bottom surface and to protect the surface in this way. A typical aerator section is shown in Fig. 4.6.

The regions of flow in the aerator are:

A An approach zone

B A transition zone beginning at the start of the bottom ramp.

C An aeration zone, the region between the downstream end of the ramp and the reattachment region. This region may be subdivided into (a) a region where no air has reached the central part of the jet, and (b) a region where air is found throughout the section of the nappe. The latter region may not exist.

D The reattachment zone, a complicated flow region near the impact point and the maximum pressure point on the spillway surface. The high pressure gradients in this region cause a rapid changes in the air distribution. It is therefore a region in which the distribution of the air changes markedly. Only at low Froude

Numbers is the flow in this region well understood. In this case a roller forms under the jet, and some of the air is entrained in this roller region.

E The zone downstream in which the turbulent flow gradually distributes the air.

Finally, continuity of air flow in the main duct requires a continuous supply of air to the space beneath the nappe. The head losses in the side duct together with the pressure change caused by the velocity change in the main duct result in the space under the nappe being at a variable subatmospheric pressure.

A The Approach Zone

In the approach zone the mean velocity will largely depend on the vertical distance from the crest, and the velocity distribution will be a function of the longitudinal distance from the crest. This latter will govern the depth of the boundary layer at the aerator. Two characteristic levels of turbulence occur, one appropriate to the boundary layer and one appropriate to the flow outside the boundary layer. Air entrainment in this zone may take place at the upper surface but only if the diffusion of air bubbles due to the turbulence at this surface is sufficient to overcome the bubble rise velocity caused by the hydrostatic pressure gradient. This condition normally occurs only if the boundary layer has reached the surface (Chapter 3), and such aeration is unlikely to be important at the first aerator.

B The Transition Zone

The transition zone coincides with the length of the ramp or deflector. This ramp is flatter than the spillway slope and is shown schematically in Fig. 4.6. At the beginning of the ramp the pressures increase above hydrostatic but reach the value of the cavity pressure at the end of the ramp, normally subatmospheric. In addition the flow depth will change over the length of the ramp; the

boundary layer becomes thinner giving a larger shear stress on the spillway floor, and the level of turbulence both inside and outside the boundary layer changes.

C The Aeration Zone

The aeration zone begins where the fluid leaves the ramp. The exact mechanism of aeration is unclear but two major differences occur between this zone and those upstream. Firstly the pressure gradient changes from hydrostatic to a much smaller but definite gradient in the opposite direction. The numerical results of Wei & De Fazio (1982) illustrate this change as do the model measurements of the pressure field obtained by Pinto (1984) shown in Fig. 4.7. Secondly the shear stress on the lower surface changes suddenly from a large value to zero. The pressure change has several effects all of which probably contribute to the air entrainment, but the magnitude of each contribution remains unknown.

For the case of zero underpressure, the flow is approximately similar to that of a circular jet ejected horizontally into the atmosphere. The latter flow, for experimental velocities below those expected on prototype aerators, has been extensively studied by Ervine & Falvey, (1986). In this case no pressure gradient resists the turbulent diffusion of the air bubbles; Figure 4.8, which from this study, illustrates the jet behaviour. It shows that the jet surface breaks up if the root mean square value of the lateral turbulent fluctuation $[v']^2$ is greater than $4\sigma/\rho R$ where R is the radius of the surface disturbance. In spite of the small scale these experiments give an insight into the flow mechanism.

Firstly the roughness from the spillway aerator and the turbulence it creates make the length before $[v']^2 > 4\sigma/\rho R$ very small. Thus, if the Weber number is large enough, the results are likely to be independent of this Number.

Secondly the under pressure will affect the jet trajectory and the local air entrainment. As the jet breaks up there is a proportion of the flow which is in the region where the pressure is the same as the closest uniform region [atmospheric pressure for the region above the nappe and the underpressure for the region below the nappe] and that which is in the region where there is a pressure gradient. In the uniform pressure region there will be droplets surrounded by air and outside this region there will be air bubbles surrounded by water.

The force due to the pressure gradient can affect only the latter region. As the jet breaks up into droplets the upper and lower nappes move closer together. Thus the depth of fluid which is affected by the pressure difference between the upper and lower nappe decreases, the effect of the pressure difference becomes more pronounced and the curvature of the trajectory increases.

Droplets detached from the jet move into a region of constant pressure and are therefore no longer subject to the jet pressure gradient. If drag is ignored their trajectory is then flatter than that of the jet, so that the droplets would return to the jet for the lower nappe surface and depart from it for the upper surface. Consequently the spray area above the nappe is greater than it is below the nappe.

If a pressure difference between the two interfaces exists, then the air bubbles will not only be moved by diffusion but will also be forced down the pressure gradient. A pressure below the nappe which is subatmospheric should then have the effect of

(a) Decreasing the air entrainment on the lower side of the nappe.

(b) Increasing the existing air entrainment at the upper surface of the spillway flow if the turbulence is sufficient. If entrainment has not commenced, the pressure gradient should increase

the possibility of commencement of air entrainment (i.e. it should start at a lower relative turbulence). This fact is consistent with Pinto (1984) observations on prototype spillways.

Finally the velocity distribution at the aerator lip will not be similar to that of an axisymmetric jet and the change from the pressure distribution at the lip to the zero pressure downstream implies a change in the velocity distribution and, in the region of the lower surface, an increase in the shear. This shear may dominate the pressure gradient effects.

D The Zone of Reattachment

The zone of reattachment is a mixing region and also a region in which the pressure gradient is greater than hydrostatic. The high pressure gradients in this region cause rapid changes in air distribution. It is therefore a region in which the air concentration distribution changes markedly. Only at low Froude Numbers is the flow in this region well understood. In this case a roller forms under the jet, and some of the air is entrained in this roller region.

E The Zone in which the Air is Gradually Redistributed

In the air distribution zone, the pressure gradient returns to hydrostatic and the air concentration in the vicinity of the chute bottom diminishes as air bubbles rise to the flow surface. However, Volkart (1985) and others show that this special rise velocity of the bubbles in a turbulent high velocity mixture is less than that in still water. When this redistribution has lowered the concentration to an unacceptable level, another aeration device must be constructed.

As prototype measurements are so difficult to perform, and because surface tension affects the results obtained in model studies, several key questions on the topic of forced aeration remain unanswered.

How does bottom aeration influence mean flow velocity?

No prototype data on velocities in aerator-equipped spillways are available. However, the addition of air during the nappe trajectory results in an increased flow depth which should be considered when designing side wall heights.

The measurements in Fig. 3.10 for an aerator free chute show that the presence of air near the concrete spillway surface either decreases the friction factor or the internal turbulent energy. Thus, conditions downstream of the aerator change in ways that are important in the design of energy dissipators. In the case of a flip bucket which throws a free jet into a downstream basin the higher velocity would change the jet trajectory.

Does the free surface aeration help in preventing cavitation?

Measurements on some models suggest that surface air entrainment at aerators may supply a considerable quantity of the air in the redistribution zone and therefore may assist in retaining an effective concentration level at the spillway floor.

4.4 AERATOR MODEL STUDIES

4.4.1 Dimensional Analysis

The foregoing discussion indicates that many physical phenomena affect aerator performance. For a model study of the complete spillway (Fig. 4.9) to determine the air demand [Q_a] through the duct, the length and velocity scales are defined as a water depth, h and the mean velocity u_w. Equation 1.2 then becomes

$$\frac{Q_a}{Q_w} = f\left[\text{geometric ratios}, \frac{k_s}{h}, Fr, Re, We\right] \qquad 4.3$$

In this relationship, the turbulence number T_u of equation 1.2 has been replaced by the k_s/h, and the pressure coefficient has been omitted since the underpressure and its distribution is determined by the inlet and duct geometry.

If the effects of the Reynolds and Weber numbers are to be negligible, the model scale must be large and this normally requires the use of a slice model representing a short section of the spillway near the aerator. For this slice, the approach conditions are not necessarily correct, and an additional length scale, the boundary layer depth (δ), and a measure of the turbulence above this boundary layer (T_u) must be introduced. Furthermore, the underpressure is controlled by a valve; the equation then becomes:

$$\beta = \frac{q_a}{q_w} = f\left[\text{geometric ratios}, \frac{k_s}{h}, \frac{\delta}{h}, T_u, F_r, \frac{2\Delta p}{\rho u_w^2}\right] \qquad 4.4$$

and can also be written as $1/E_u^2$ where E_u is the Euler Number. The pressure coefficient $\left(2\Delta p/\rho u_w^2\right)$ can be combined with the Froude Number to yield a pressure gradient number $\Delta p/\rho gh$ and the equation can be written

$$\beta = f\left[\text{geometric, ratios}, \frac{k_s}{h}, \frac{h_b}{h}, Fr, \frac{\Delta p}{\rho gh}\right] \qquad 4.5$$

The results from these slice models can be integrated to obtain a result for the full width of the prototype.

4.4.2 The Air Demand Curves

In some of the early investigations Pan (1980), Pinto (1978), Wood (1984) suggested that the air entrainment for several specific aerators was a simple function of the dimensionless length of the trajectory of the nappe [L] of the type

$$\beta = \frac{q_a}{q_w} = K\left[\frac{L}{h}\right] \qquad 4.6$$

Indeed tests show, that for a given aerator geometry, chute slope, underpressure and Froude Number, the linear relationship between air entrainment and dimensionless jet length applies to some aerators. The results are, however, not generally applicable.

Later analyses have been more general. If the air supply is unlimited [i.e. the pressure under the nappe was atmospheric], the air

demand curve for given upstream conditions is a unique function of the Froude number. For this case the variation of the air demand curve [β] with the Froude Number was determined by Rutschmann (1985) and Koschitzky (1987). Rutschmann made measurements on a chute with a slope of 49% and with a ramp of 200 mm length, an inclination tanϕ of 12% and an offset of 66 mm. In this test series the influence of the subpressure was eliminated by boosting the ventilation system of the aerator with a blower in order to reach a zero subpressure. Figure 4.10 shows that for this case for Froude numbers greater than about 6.2 (for the given geometry) the relation between β and Fr is linear. Koschitzky's results were similar. For this linear range entrainment is expected along the full length of the underside of the nappe. The departure from the straight line in the region of lower Froude numbers was probably caused by a change of the entrainment mechanism.

Wood (1984), Tan (1984), Rutschmann (1985), Low Heng Seng (1986), Volkart and Rutschmann (1986) and Koschitzky (1987) showed that, for a given Froude number, pressures below atmospheric in the region below the nappe reduced the value of β. Indeed Rutschmann's measurements of β on the Clyde Dam model (Fig. 4.12) showed that the change in the mechanism discussed above occurred for high subpressures but the transition Froude number was larger than in Fig. 4.12. At the higher Froude numbers the rate of increase of β with Froude number is expected to be smaller and β will reach a maximum value. The results obtained for the particular geometry of the Clyde chute

are approximated by the following empirical equation:

$$\frac{q_a}{q_w} = \beta = K_1 \left(Fr - K_2\right) - K_3 \left(\frac{\Delta p}{\rho_w g h} \right)^{\gamma} \qquad 4.7$$

or

$$= K_1 \left(Fr - K_2\right) - K_3 \left(Fr^2/Eu \right)^{\gamma} \qquad 4.7(a)$$

where K_1, K_2, K_3, and γ are constant factors for a given aerator geometry and Δp = atmospheric pressure minus the pressure below the nappe. Figs. 4.11 - 4.14 show the results obtained for a ramp without offsets.

The results show that the air demands for the different geometries differ considerably. For the smaller ramp and offset heights, the subpressures are considerably higher. This result can be explained from a consideration of the jet trajectory. For high specific discharges the jet deflection angle at the end of the ramp no longer equals the ramp angle but is somewhat smaller. For this case, particularly if the ramp lip is not sufficiently distant from the downstream chute, the jet length and therefore air entrainment may be drastically reduced. In an extreme case the aerator could be immersed, and would then act as a cavitation generator.

No systematic study of the effect of upstream roughness [k_s/h], the free stream turbulence, T_u or of the relative boundary layer depth δ/h is available. Preliminary studies do, however, show that increasing k_s/h increases the air demand.

Prototype performance is difficult to measure and therefore data are rare. The data that exist are useful in the design of aerators and are analyzed in chapter 5.

4.4.3 Jet Trajectory Calculations

A calculation of the jet trajectory gives additional design information about the position of impact (important for the aerator spacing) and the necessary height of the spillway side wall. The results supplement information obtained from hydraulic models. Two approaches have been used in the past.

(1) If the surface tension is neglected and the ramp is long enough for all the fluid leaving the ramp to be parallel to the ramp slope, then the method of Schwartz and Nutt (1963) is applicable. They use the one-dimensional equations of continuity and motion and derived the following expressions for the jet coordinates:

$$\frac{y'}{h_o} = \frac{Fr_o^2 \sin\theta_o}{a \sin\gamma_o} \left[\cos\gamma_o - \cos\left(\frac{u_o at}{Fr_o^2 h} + \gamma_o\right)\right] \qquad 4.8$$

$$\frac{x'}{h_o} = -\frac{u_o t}{a h_o} + \frac{Fr_o^2 \sin\theta_o}{a \sin\gamma_o}\left[\sin\left(\frac{u_o a t}{Fr_o^2 h_o} + \gamma_o\right) - \sin\gamma_o\right] \qquad 4.9$$

with $a > 0$.

The following additional symbols and abbreviations are used (see Fig. 4.14).

Fr_o	[-]	Froude number at the ramp
h_o	[m]	flow depth at the ramp
t	[s]	time
u_o	[m/s]	initial velocity at the ramp
x'	[m]	co-ordinate in horizontal direction
y'	[m]	co-ordinate in vertical direction
θ_o	[-]	initial angle of the trajectory to horizontal = $\alpha - \phi$
a	[-]	$\frac{\Delta p}{\rho_w g h_o}$
γ_o	[-]	$\tan^{-1}\left[a \cos\theta_o / \left(a \cos\theta_o + 1\right)\right]$

The solution of these equations shows that a small subatmospheric pressure under the nappe markedly affects the nappe trajectory.

(2) If the ramp is short and the upper fluid surface is not parallel to the ramp then the complete two dimensional equations of motion can be solved. (Wei. and De Fazio 1982.)

For most purposes, however, the first approach is adequate. An attempt to modify this approach and to allow for the influence of the non parallel flow over the ramp is described in Pan et al. (1980).

4.4.4 Air Concentration Downstream of an Aerator and Air Slot Spacing

Air concentrations downstream of an air slot and near the channel bottom are of primary importance for cavitation erosion protection. At the point of impact of the unaerated core of the jet the bottom air concentration is very low. But at the position where the aerated nappe reaches the bottom, and also just downstream of the mixing zone, concentration rises to a maximum value.

Figs. 4.15 - 4.19 show model measurement of air concentrations downstream of the aerators. Through the nappe and upstream of the point of impact of the jet there may be two regions of air concentration, one from the surface aeration and one from the aeration under the nappe. Depending on the aerator geometry these two regions may merge as shown in Fig. 4.15.

Downstream of the point of impact the hydrostatic pressure distribution is re-established and turbulence in the flow redistributes the air bubbles, Fig. 4.17. On spillways with relatively flat slopes this redistribution is marked; Figs. 4.18 and 4.19 show examples of concentration distributions along the channel bottom with a slope of 0.140.

For the steeper slopes this redistribution of the air is much less apparent. In both cases the mean air concentration and air concentration distribution must tend to the distribution appropriate to the particular slope. [Chapter 3.] Should the air concentration near the channel floor fall below the amount necessary to protect the spillway from cavitation then a second aerator must be installed.

The maximum length protected by each aerator cannot be determined, but it will depend on the velocity and slope. Some insight into the air redistribution processes can probably be gained from papers dealing with a diffusion model for a de-aeration zone (Nokes, 1985) or from measured prototype concentrations within a redistribution zone (Volkart, 1985).

Perhaps the best information on this variable comes from prototype experience, and Appendix 1 contains information on selected present designs. These however must be used with caution as few will have had their maximum spillway discharge.

4.4.5 Scale Effects

Firstly, although the correct model discharges and depths are produced upstream of the ramp the model velocity gradient next to the spillway floor may not be correct (Volkart, Rutschmann, 1983); also the roughness and hence the local boundary layer turbulence are difficult to scale correctly. Pinto (1984) and Ervine and Falvey (1986) show that

roughness (k_s/h) affects the onset of the instabilities on the lower nappe and can have a marked effect on the entrainment. The turbulence above the boundary layer is also unlikely to be correctly reproduced, and it is suggested that tests should be carried out for a range of velocity distributions.

Secondly, the bubble sizes in the flow are certainly not correctly scaled. Finally, in modelling a relatively small slice of the spillway the boundary layers on the side-wall occupy a much larger proportion of the flow than they do on the prototype. Figs. 4.18 and 4.19 illustrate the marked difference in the air concentrations at the model centreline and close to the model walls. The drag on the side walls and the resultant lower velocities cause the jet to first reach the floor near the wall. Thus the maximum air concentration is nearer the air duct than it is to the centreline.

4.5 AERATOR SUPPLY SYSTEM CALCULATIONS

A schematic of the air flow in main and side duct is shown in Fig. 4.20. At the entrance of the main duct the pressure is subatmospheric by an amount equal to the head loss in the side duct and the velocity head. At the centreline of the main duct the subatmospheric pressure is the head loss in the main and side ducts. [The velocity head is recovered, friction losses in the main duct are neglected and the flow in the main duct is assumed to be uniform.]

The pressure loss through the side duct Δp_c in the spillway sidewall is written as

$$\Delta p_c = K_s \frac{1}{2} \rho_a \left[\frac{Q_{Ta}}{A_{sd}} \right]^2 \qquad 4.10$$

where ρ_a = air density

Q_{Ta} = the total air flow

A_{sd} = area of the side or inlet duct

K_s = the head loss coefficient for the side duct (estimated from D S Miller, 1978, or I.E. Idel'cik, 1969).

Typical values for K_s for a bell shaped inlet and rounded 90° bend in the air shaft, 1.0 for a rectangular inlet area without a bell mouth and with rounded 90° bend and 2.0 for a rectangular inlet area without a bell mouth and without a rounded 90° bend.

Assuming that the average pressure beneath the nappe be equal to the pressure loss through the side ducts, i.e. that pressure variations in the cavity due to changes in the velocity head be only a locally restricted phenomenon, equation 4.10 with the average pressure $\overline{\Delta p}$ replacing the pressure loss Δp_c can be written:

$$Q_{Ta} = \sqrt{\frac{2\overline{\Delta p}}{K_s \rho_a}} \cdot A_{sd} \qquad 4.11$$

and in combination with $Q_w = uhB_e$ the terms can be regrouped as follows:

$$\beta_t = \frac{Q_{Ta}}{Q_w} = \frac{A_{sd}}{B_e h Fr} \cdot \left[\frac{2}{K_s} \frac{\rho_w}{\rho_a} \frac{\Delta p_c}{\rho_w g h} \right]^{0.5} \qquad 4.12$$

For a given Froude Number the aerator rating curve is known [Figs. 4.12 - 4.14] and this curve can be combined with an equation for the air demand (similar to 4.7) to explore the effect of changing the nondimensional side duct area. [Fig. 4.21]

Further, if the transverse pressure variation in the main duct as measured by Pinto (1982) is taken as typical then

$$\overline{\Delta p} = 0.43 \left(\frac{1}{K_s} + 2 \right) \Delta p_c \qquad 4.13$$

and equation 4.12 can be written as

$$\beta_T = \frac{A_{SD}}{B_e h} Fr \left[\frac{\rho_w}{\rho_a} \frac{2\overline{\Delta p}}{K_s \; 0.43 \left(1/K_s + 2 \right)} \rho_w g h \right]^{0.5} \qquad 4.14$$

Finally if the following approximations are acceptable

4.18

(1) The effective area A_d in which the air is flowing along the duct is approximately constant and can be estimated. The entrance into the area beneath the nappe can be taken as this cross-section.

(2) The air flow in the duct is one-dimensional and thus the velocity does not vary with position in the duct cross-section.

(3) The duct under the aerator is sufficiently short that the head loss in this portion of the flow is negligible; thus the pressure head increases as the discharge decreases.

(4) The friction loss is negligible but the change in the subpressure due to the change in the velocity head along the duct is important.

Then the Bernoulli equation written from the atmosphere to any position x in the duct [Fig. 4.20] yields

$$Q(x) = \left(\frac{2\rho_w g h \Delta p_*}{\rho_a} \right)^{0.5} \qquad 4.15$$

where $\Delta p_* = \left(\Delta p(x) - \Delta p_c \right) / \rho_w g h$

Differentiating 4.14 and dividing by q_w and substituting for q_a/q_w from 4.7 yields

$$K_1 \left(Fr - K_2 \right) - K_3 \Delta p_*^{\gamma} = \frac{A_d}{h} \left[2 \frac{\rho_w}{\rho_a} \frac{1}{Fr^2} \right]^{0.5} \frac{1}{\Delta p_*^{0.5}} \frac{d\Delta p_*}{dx} \qquad 4.16$$

If the centreline pressure difference (i.e. the pressure where there is no flow along the duct) is assumed then equation 4.16 can be integrated numerically to obtain the pressure distribution along the duct. The local air demand can then be computed and the integration of this demand gives the total air flow. The total air flow then enables one to estimate the centreline pressure difference due to the head loss in the inlet ducts in equation 4.11). The process can be repeated until the computation of the centreline pressure difference is within the desired accuracy. From these calculations the value of β at positions along the duct can be computed.

For $\gamma = 1$ an analytic solution can be obtained, Rutschmann, Volkart and Wood (1985). The above numerical method could also be used for the case where the friction losses in the ducts are included. However, these will be small if the ducts are large.

For an aerator with an air demand function with the constants similar to those obtained for Foz do Areia (Pinto 1984). $K_1 = 0.173$, $K_2 = 4.94$, $K_3 = 1$ and an inlet loss which yields a value for K_s of 0.536. The results are shown in Fig. 4.22. This figure shows that increasing the dimensionless duct area $\left(A_d/L^2\right)$ yields an increase in the dimensionless air demand and greatly improves the uniformity of the airflow over the duct length.

4.6 The Aerator Shapes

Only a few aerator shapes are feasible as they must fulfil the following conditions:

(1) Entrain large quantities of air, with an air concentration that is well distributed and high at the most endangered surfaces along the length of a chute, i.e. having a large value of β at small underpressures.

(2) The rate at which the value of β falls with increasing $\Delta p/\rho_w gh$ should be acceptably small.

(3) The main duct area should be as large as feasible.

(4) Have a simple and economic design and yet prevent any erosion damage to the device itself.

The foregoing conditions result in the use of deflectors, offsets, grooves and combinations of these as shown in Fig. 4.23.

These elements are usually placed at the bottom of the spillway. However, if additionally installed at the side walls of the chute, they can also replace a special aeration system by creating space for air supply to the bottom cavity. The three air slot types, namely deflectors, offsets and grooves all work in a similar manner. However, the special geometry of each device implies different air demand curves.

The first deflectors were prefabricated from steel and have been used as remedial measures on existing spillways. Their height ranged from 0.10 to 1.00 m. An advantage of this air entrainment device is that even with small deflector heights an underjet space of considerable length is created, however, the increased velocities due to the ski jump effects results in increased shock wave production.

If aeration is anticipated at the outset of the design stage, offsets may be incorporated in the design. These have the advantage of minor shock wave disturbance, an enlarged jet trajectory at higher discharges and - above all - enough space for air supply.

Grooves, which are often used in tunnels or after gates, have the advantage of ease of air supply. This supply comes either from special air vents or from a free air space produced by the placing of aeration devices on the spillway side walls. Grooves are usually 1.00 to 2.50 m deep. The main disadvantage is their small air demand due to the small exposure of the nappe to the air. Most grooves are therefore combined with either an offset or a deflector or both an offset and a deflector.

Recent experience has tended to favour a combination of offset and deflector as the most practical aeration device.

Engineering design practice combines the aerators with discontinuities in the chute's longitudinal profile. Therefore, locations of the aerators are given, and an adequate aerator geometry has to be designed in order to guarantee sufficient floor aeration. Figure 4.24 shows some of the possibilities: (a) and (b) show the transition from a flatter to a steeper slope. Type (a), provided the cavity and the jet length are large enough, may even be used to avoid a ramp or a step. For a transition from a steeper to flatter slope a ramp is recommended; (c) is a tested configuration with a curved ramp.

4.7 The Inlet Duct System

Inlet duct systems are usually designed for low head loss. In this way the subatmospheric pressure under the nappe is small, and the

efficiency of the aerator is high. To date a large number of different prototype air supply systems have been built [Fig. 4.25(a), (b), (c), (d) and (e)].

The inlets are either:

(1) through a cavity created by a geometric discontinuity at the spillway walls, [Fig. 4.25(a),(b), (c) and (d)], or by

(2) special air shafts or conduits built into the spillway [Fig. 4.25(e)].

The aerator illustrated in Fig. 4.25(c) is often used for the aerator closest to the crest. For the others the one illustrated in Fig. 4.25(e) is the most common design.

4.8 A Suggested Design Procedure

Every project is unique; nevertheless, the following procedure may assist an engineer in optimising various aspects of the hydraulics, construction, maintenance, safety and economy of a spillway.

For each spillway some parameters can be considered as given. These are:

- the slope and size of the upper approach flow area including head works;
- the chute's longitudinal profile;
- the chute's width;
- the most frequent discharge and the maximum possible discharge, and, consequently, the maximum specific flow rate;
- an attainable quality of concrete and its surface roughness.

The following design procedure is recommended:

1 **Determination of the mean flow velocity along the whole chute.**

The mean flow velocity can be determined either from a computed backwater curve or from a general hydraulic model with a scale of between 1:50 and 1:100. Computer calculations (Chapter 3) can be adjusted to include various surface roughness coefficients. In partial contrast, a hydraulic model reproduces the flow at the upstream approach area and

across the openings of the head works but not the effect of surface air entrainment. For non-symmetrical flow conditions for gate-regulated spillways, hydraulic model tests are almost indispensable.

2 The location of the first aerator.

The mean velocity of the flow enables both the cavitation coefficient and the critical velocity to be determined, and these should be used as a guide in determining the position of the first aerator. A minimum Froude number of about 4 is recommended. The position of the joints, changes in slope and the possibility of ventilation through the pier ends should be considered.

3 The geometry of the first and subsequent aerators.

A preliminary design can be taken from the examples in Appendix 1. However, tests on detailed hydraulic models are necessary; thus scales should be at least 1:10 or 1:15, and they should represent a reduced chute width (for instance 0.30 to 0.50 m in the model). In spite of unavoidable scale effects, the models can be used to compare the air demands for different aerator shapes with a range of flow rates and subpressures under the nappe, (i.e. the characteristics of the aerator and the duct), and to determine the jet length and jet impact angle. Velocity profiles and local air bubble concentrations in the air redistribution process can be measured. The jet trajectory from the aerator can either be computed or modelled at a very small scale (1:100). The geometry of the aerators should be such that the impact point of the jet is remote from construction joints and subsequent aerators. The aim of the design should be to produce sufficient air at the spillway surface. This implies a large but not necessarily the maximum β value. The air duct and inlet size may be determined to give a maximum air intake and uniform distribution using the method suggested in 4.5, and the velocities in the duct should be limited to the order of 60-80 m/sec. The duct must be well drained and assurances provided against the possibility of it becoming submerged.

4-2

4 **The aerator spacing.**

At present no definite guidance is available as to the required spacing. However, past designs have used spacings of 30 to 90 m.

5 **The effects of aerated flow on the inlet condition to the dissipator.**

The side walls must be high enough to account for the increased flow depth due to natural surface and aeration, the jet trajectory and surface waves. The aerated flow will affect the dissipator and indeed the reduced friction may increase the trajectory from ski jump spillway and may affect the performance of a bucket or stilling basin.

6 Concrete quality

Consideration should be given to changes in the concrete quality and surface roughness during the long operational life.

4.29

4.9 LIST OF SYMBOLS

a	[-]	a pressure coefficient $\left(\Delta p/\rho_w g h_o\right)$
A_D	[m^2]	the area of the main duct
A_{SD}	[m^2]	the area of the side or inlet duct
B_e	[m]	the effective width of the aerator
c	[-]	the average air concentration
Fr	[-]	the Froude Number
Fr_o	[-]	the Froude Number at the ramp
g	[m/s^2]	the acceleration of gravity
h	[m]	the depth of flow normal to the surface
h_o	[m]	the flow depth at the ramp
k_s	[m]	the equivalent sand grain roughness
K_s	[-]	the head loss coefficient for the side duct
L	[m]	the length of the trajectory of the jet from an aerator
p	[Pa]	the local surface pressure
p_a	[Pa]	the local atmospheric pressure
p_v	[Pa]	the vapour pressure of the water
q_a	[m^2/s]	the air discharge per unit width of spillway
q_w	[m^2/s]	the water discharge per unit width of spillway
Q_a	[m^3/s]	the air duct air demand
Q_{TA}	[m^3/s]	the total air flow
Q_w	[m^3/s]	the total water discharge down the spillway
r	[m]	the radius of curvature of the boundary
R	[m]	the radius of curvature of a surface disturbance
R_e	[-]	the Reynolds Number
t	[s]	time
T_u	[-]	a turbulence number
u	[m/s]	the flow velocity
u_o	[m/s]	initial velocity at the ramp
u_w	[m/s]	the mean water velocity
v'	[m/s]	the lateral turbulent fluctuation

W_e	[-]	the Weber Number
y'	[m]	the vertical coordinate with the ramp as origin
x'	[m]	a horizontal coordinate with the ramp as origin
α	[ ]	the angle between the spillway surface and the horizontal
β	[-]	the ratio of q_a/q_w
γ		a constant in the air demand equation
γ_o	[ ]	$\tan^{-1}\left[a \cos\theta_o / \left(a \cos\theta_o + 1\right)\right]$
δ	[m]	the depth of the boundary layer
Δp	[Pa]	the pressure difference between the underside of the nappe and the pressure above the nappe
Δp_c	[Pa]	the pressure loss through the side duct
Δp_*	[-]	$\left(\Delta p(x) - \Delta p_c\right)/\rho$
θ_o	[-]	the initial angle of the trajectory measured from the horizontal
ρ_w	[kg/m^3]	the density of the water
σ	[N/m]	the surface tension
σ_c	[N/m^2]	the concrete strength

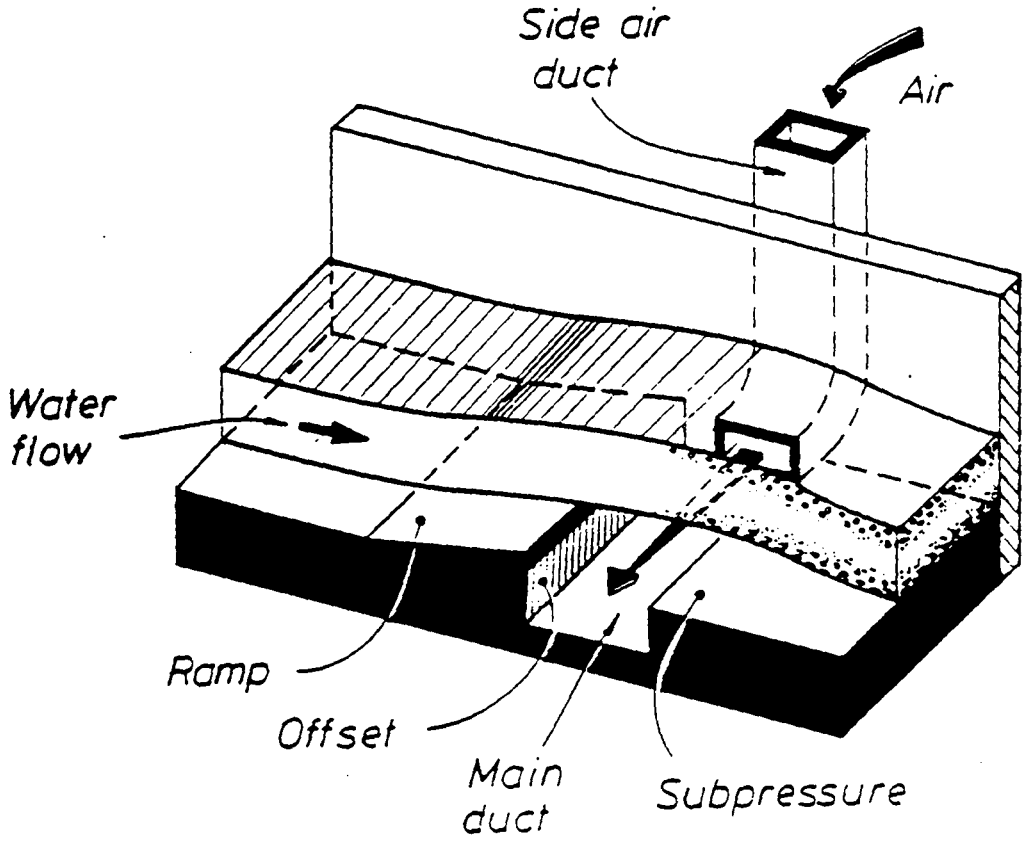

Fig. 4.1 A typical bottom aerator

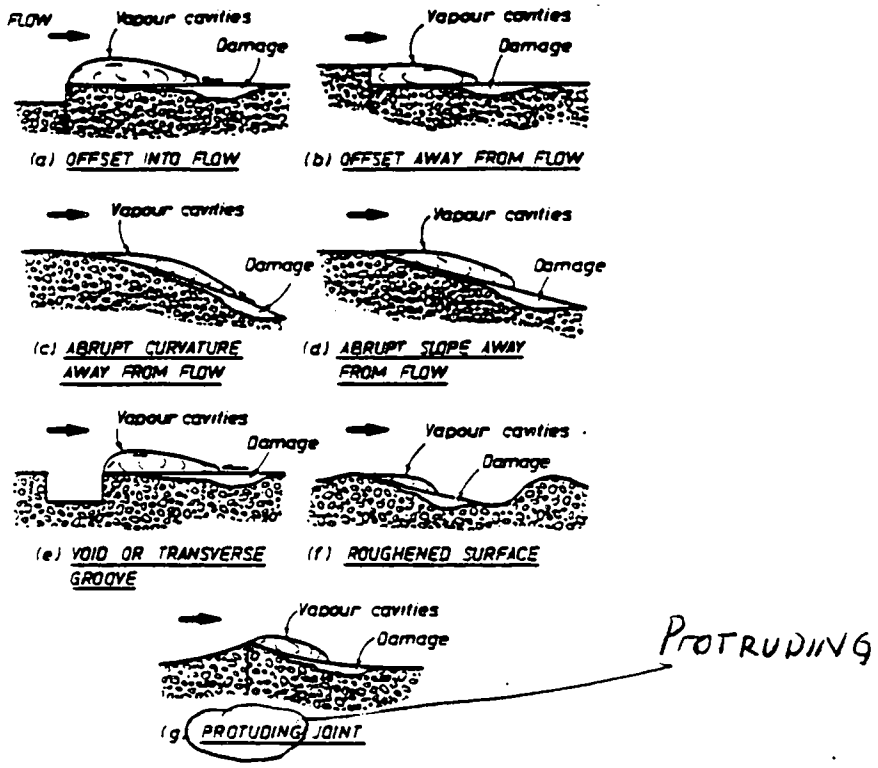

(a) The effect of surface discontinuities [Ball 1976]

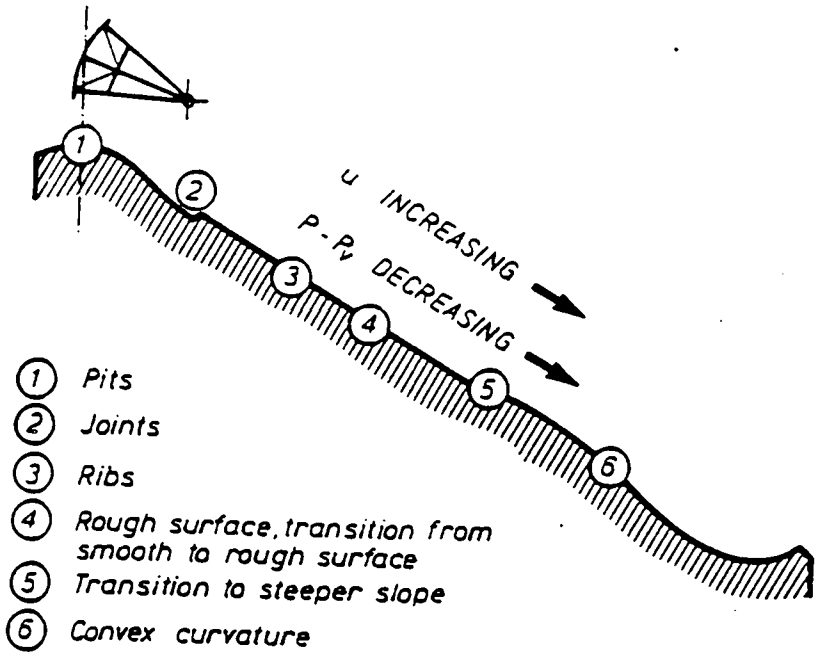

(b) A typical distribution of cavitation areas on a spillway [Volkart & Rutschmann 1984]

Fig. 4.2 Factors affecting cavitation erosion on an open chute spillway

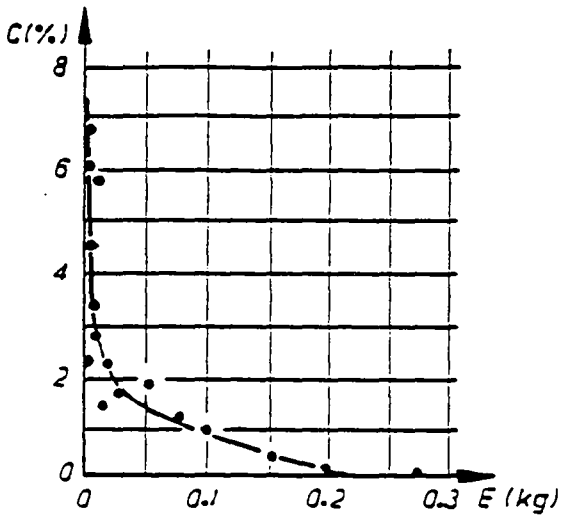

Weight loss in kg

Fig. 4.3 Air concentration versus cavitation weight loss of concrete specimens (Peterka, 1953)

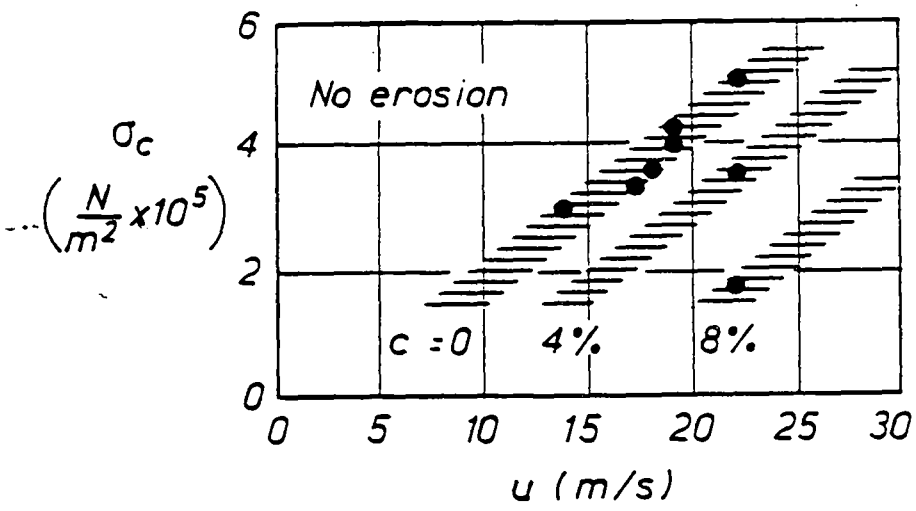

Fig. 4.4 The relationship between allowable velocities of a cavitation flow, the concrete strength σc and the air content c (Galperin et al., 1971).

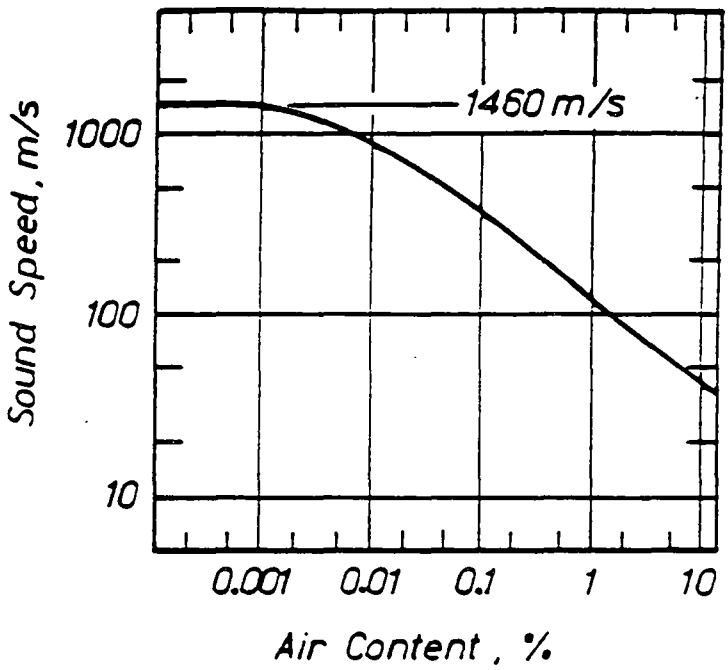

Fig. 4.5 The speed of a compression wave in isothermal surroundings. For zero air concentration this velocity is 1470 m/s, but for c = 0.5 this velocity is approximately 20 m/sec. This makes prototype flow supersonic and makes measurement with a normal probe extremely difficult. [Cain, 1978]

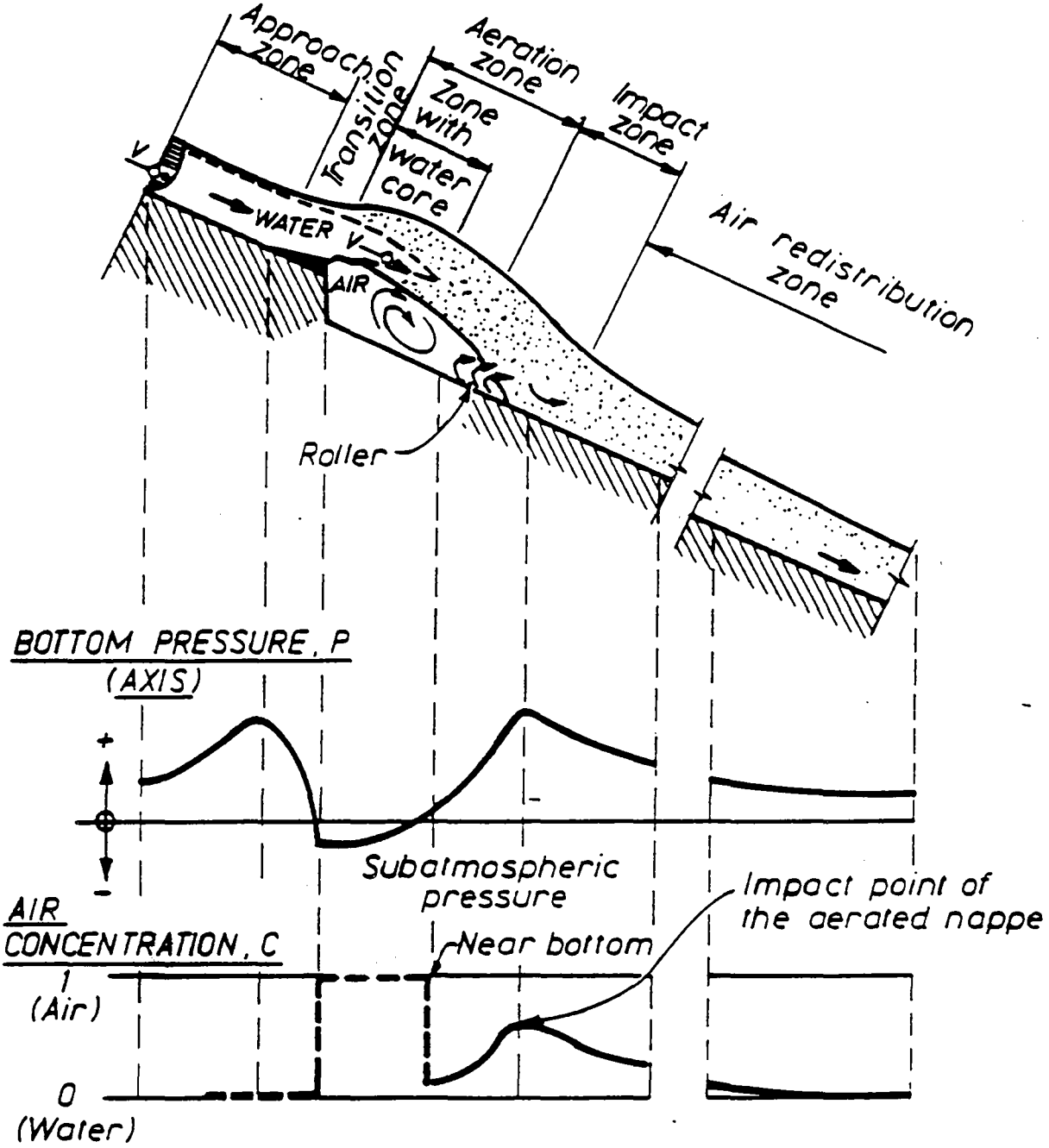

Fig. 4.6 The regions of flow for a typical aerator

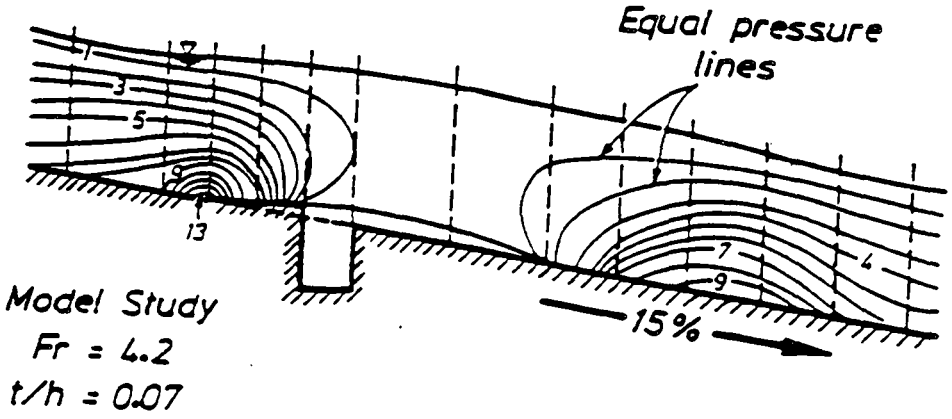

Fig.4.7 The pressure distributions at an aerator measured at the side wall on a model [Pinto, 1984]

(Note the hydrostatic distributions well upstream and downstream of the aerator and the constant atmospheric pressure in the free jet region) [Underpressure lines not measured]

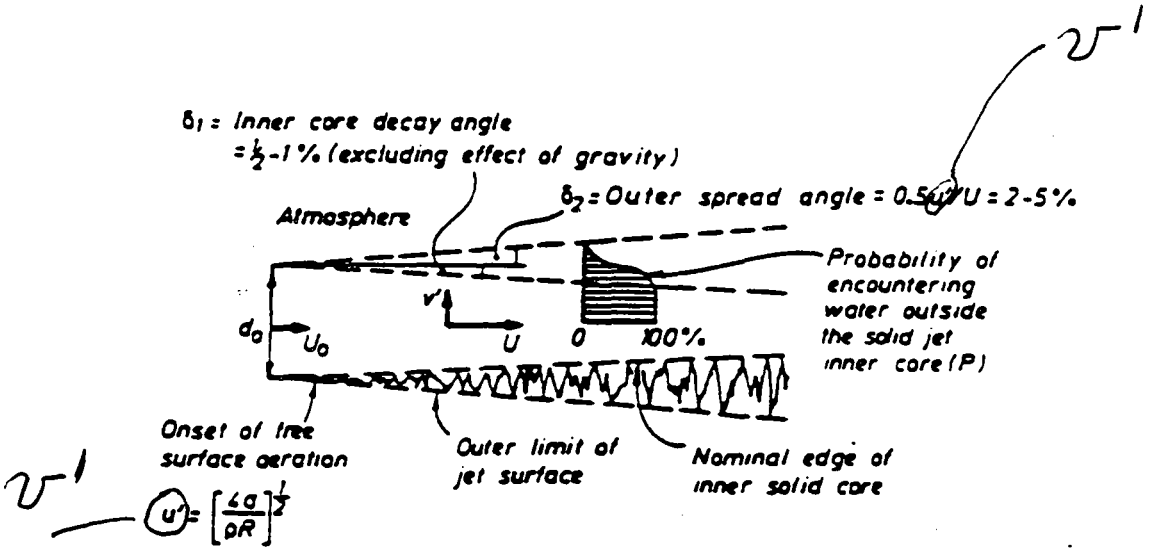

Fig. 4.8 The break up of an axisymmetric jet [Ervine and Falvey, 1986]

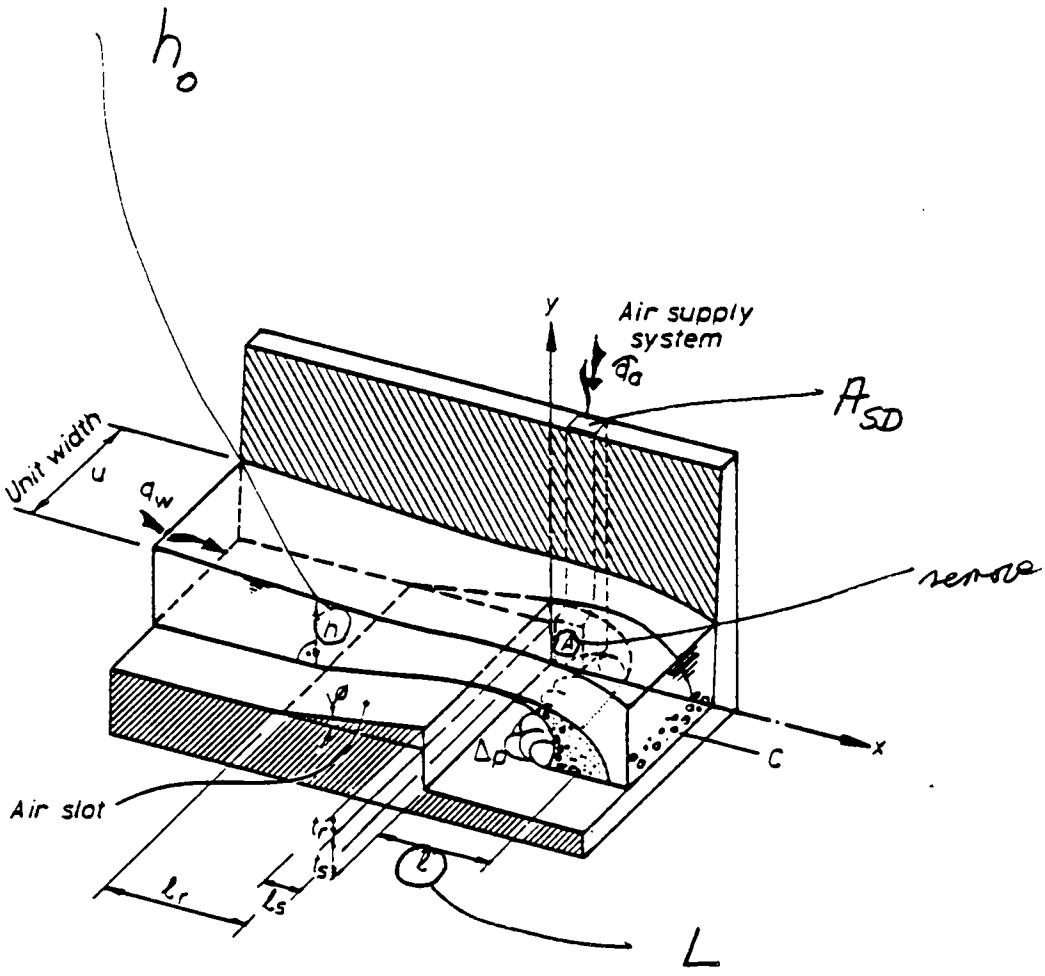

Fig. 4.9 The nomenclature for an aerator

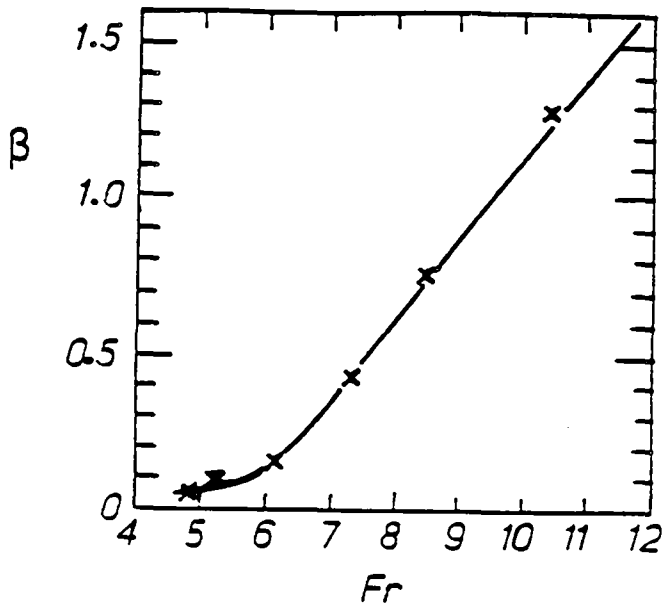

Fig. 4.10 The relationship between the Froude Number and the aeration coefficient for zero subpressure as determined by the model studies [Rutschmann, 1985]

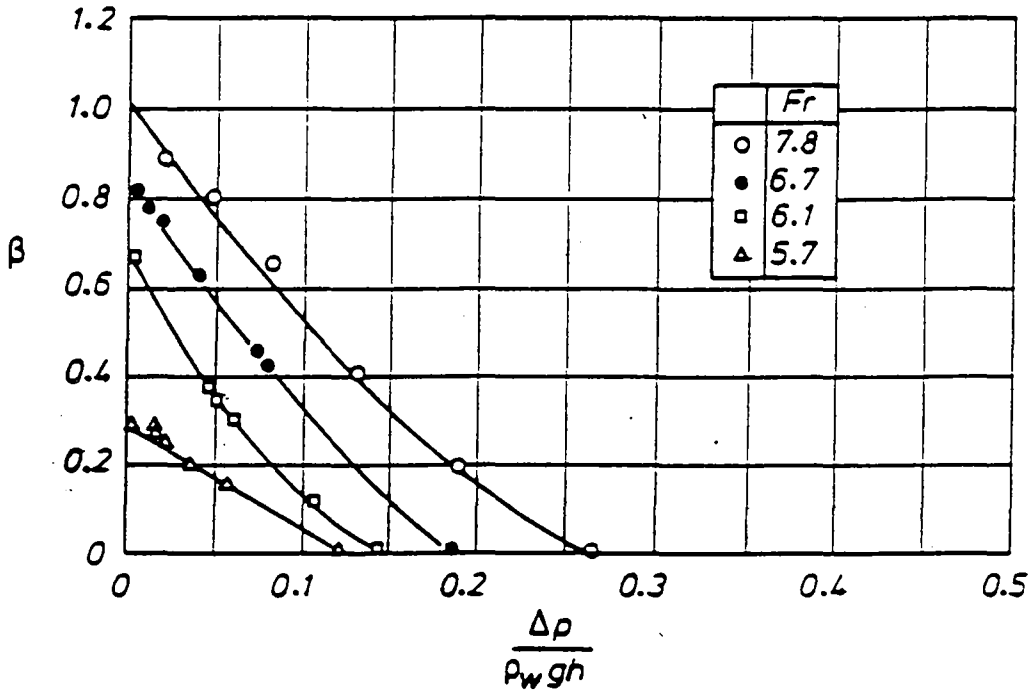

Fig. 4.11 Air demand results from the Clyde dam model with a ramp height of 39 mm (no offset).

The coefficients in equation 4.7 were determined as K1 = 0.29, K2 = 4.36, K3 = 5.02, γ = 1.17 [Rutschmann, 1985]

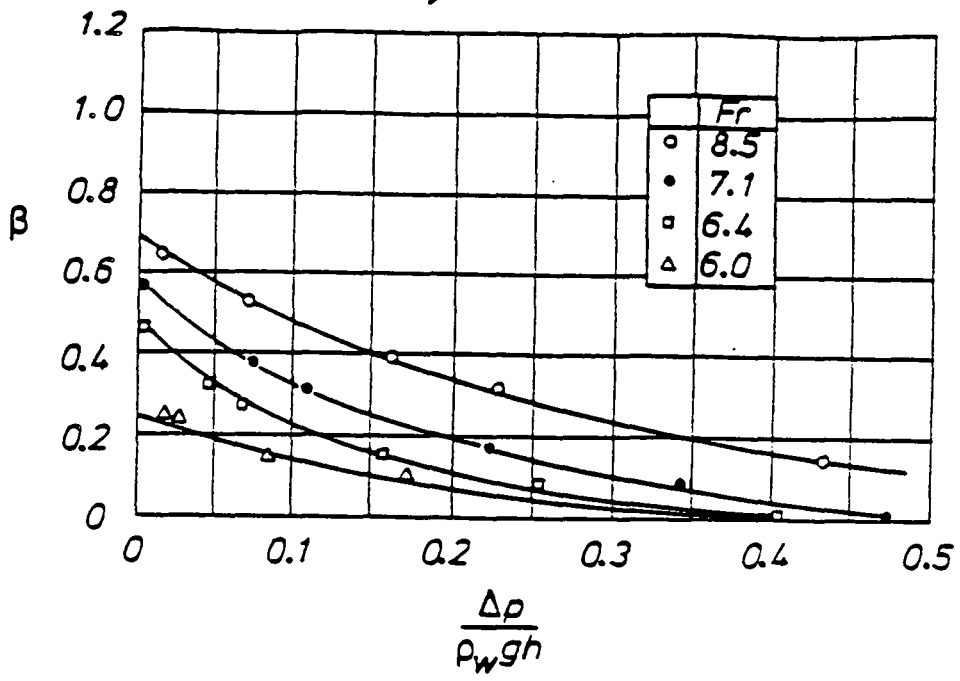

Fig. 4.12 Air demand results for the Clyde dam model with a ramp height of 23 mm (no offset).

The coefficients for equation 4.7 were determined as K1 = 0.12, K2 = 2.23, K3 = 0.80, γ = 0.48 [Rutschmann, 1985]

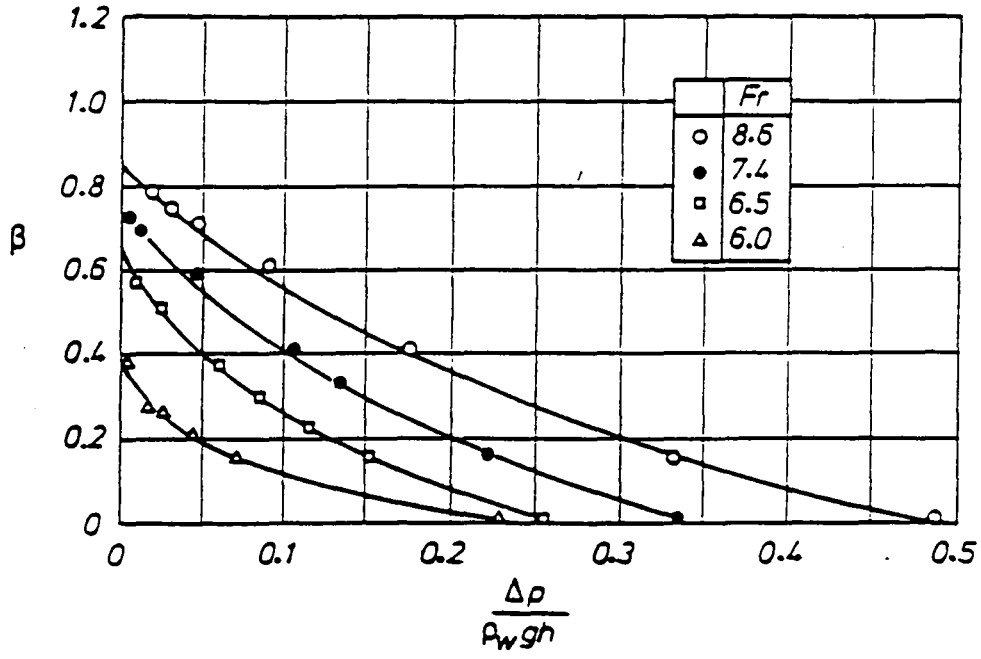

Fig. 4.13 Air demand results for the Clyde dam model with a ramp height of 30 mm (no offset).

The coefficients for equation 4.7 were determined as K1 = 0.13, K2 = 2.94, K3 = 1.14, γ = 0.84 [Rutschmann, 1985]

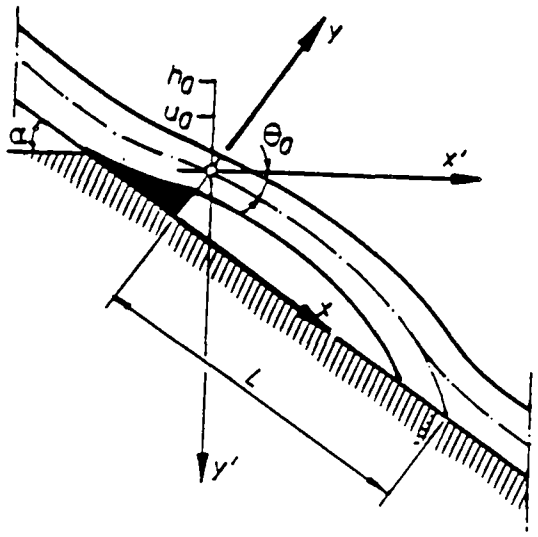

Fig. 4.14 Nomenclature for jet length calculations. Definition of co-ordinates x' and y' and the jet length L

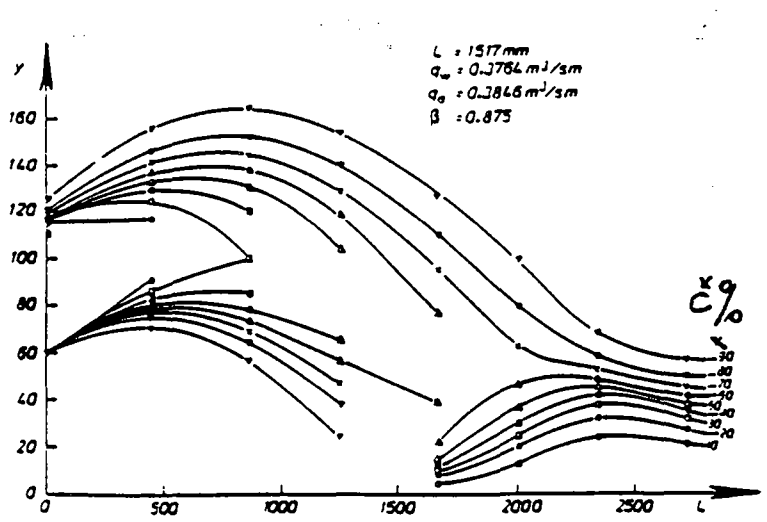

Fig. 4.15 Air concentration contours for the Clyde aerator model. The dimensions are in mm [Wood, 1984]

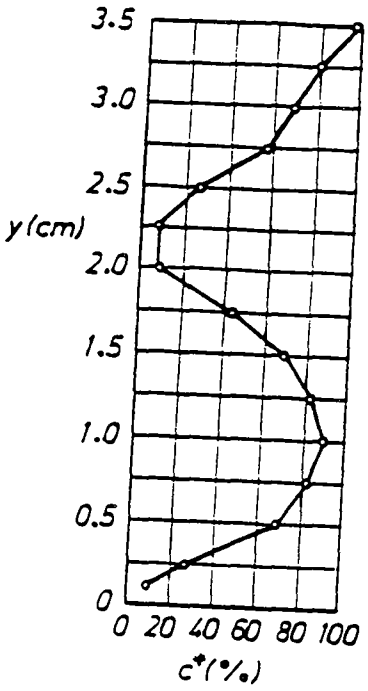

Fig. 4.16 An example of the air concentration profile for tan α = 1/4, q_w = 40 m3/ms, tr = 0.50 m, ts = 0.75 m measured in a 1:25 model (according to Vischer, Volkart, Siegenthaler, 1981. San Roque model)

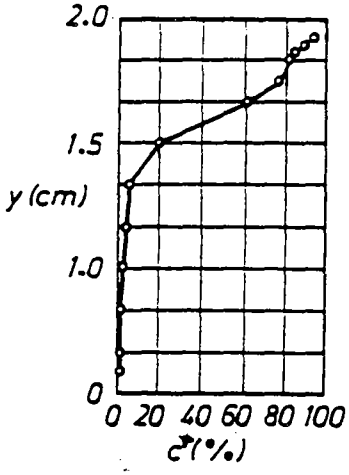

Fig. 4.17 Profile a considerable distance downstream of the air slot (model) [Vischer, 1981]

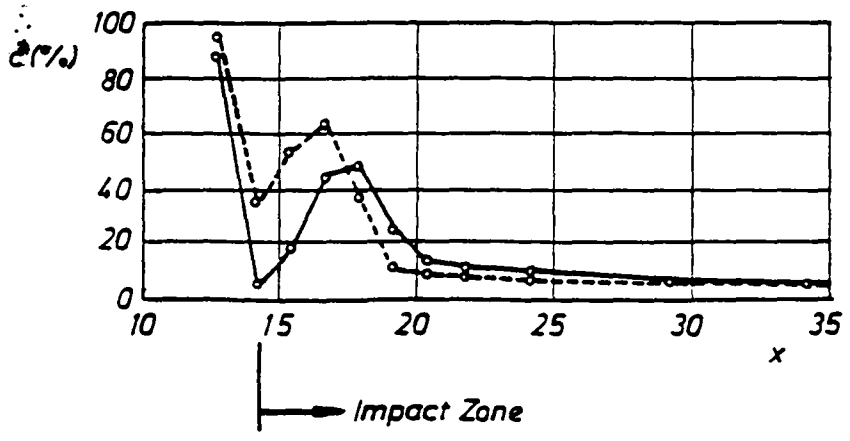

Fig. 4.18 Air concentration distribution along the channel 0.4 cm above the floor [Volkart, Chervet, 1983]

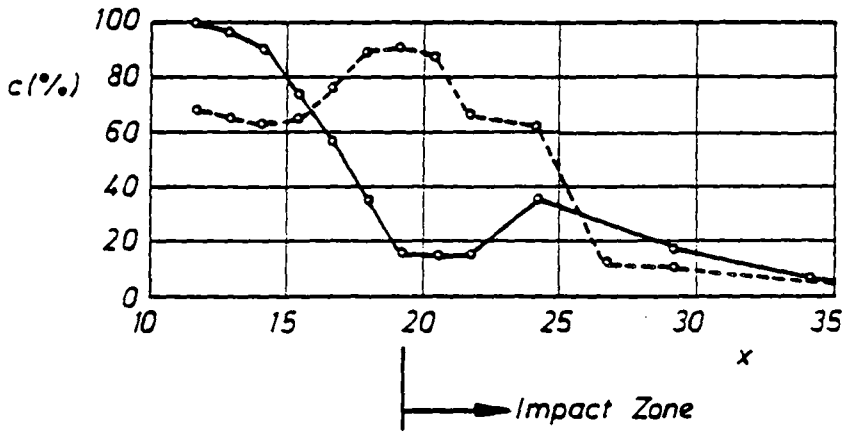

Fig. 4.19 An air concentration distribution along the channel bottom (model) [Volkart, Chervet, 1983]

4·3

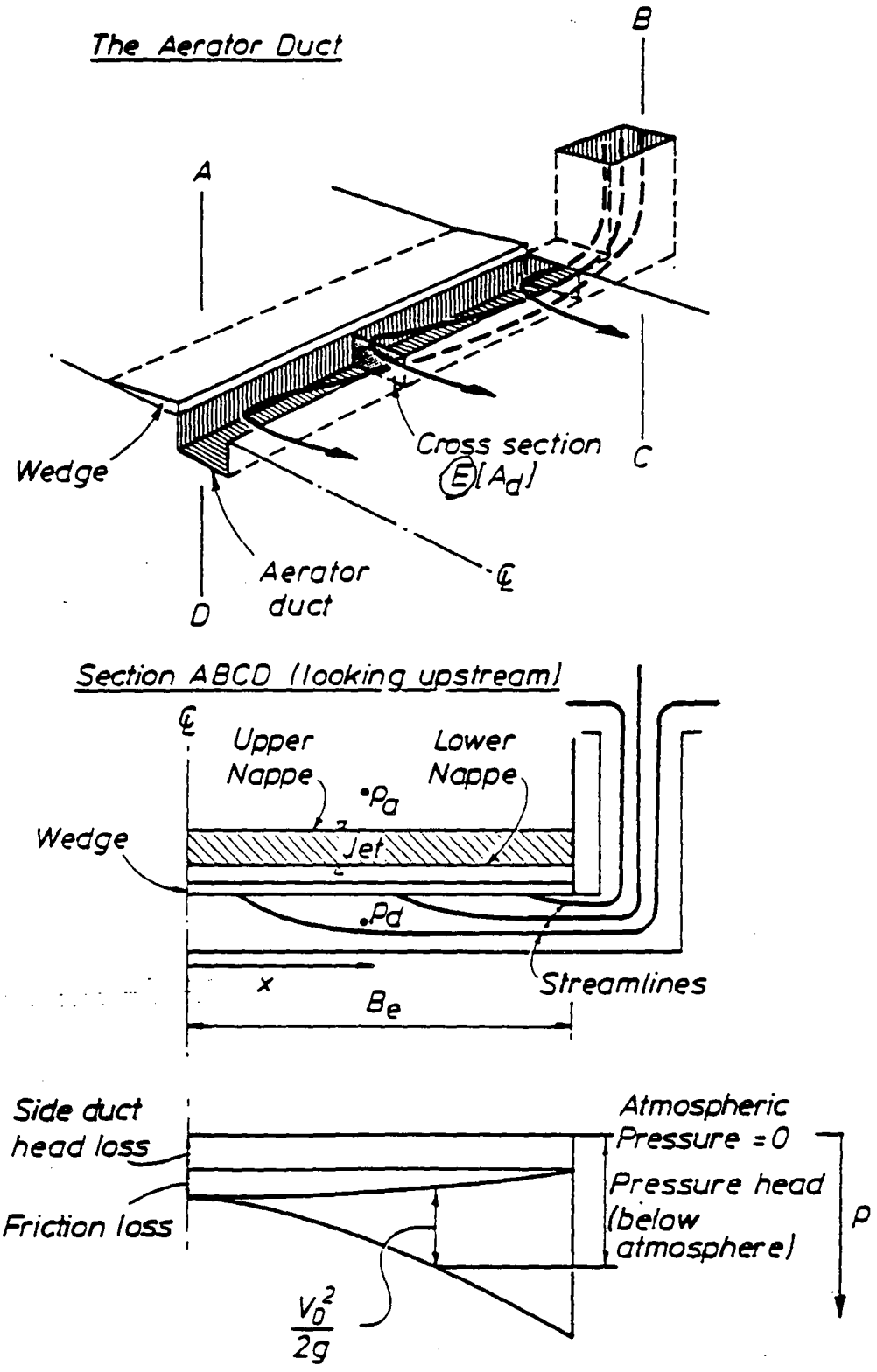

Fig. 4.20 A schematic of the flow in an aerator duct [Lov, 1986]

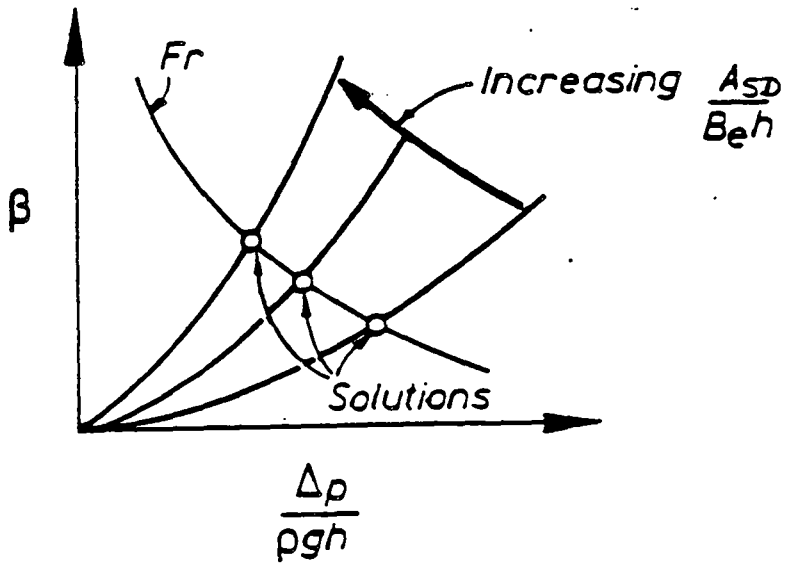

Fig. 4.21 The solutions to equations for the aerator demand curve (4.7) and the duct rating curve (4.12)

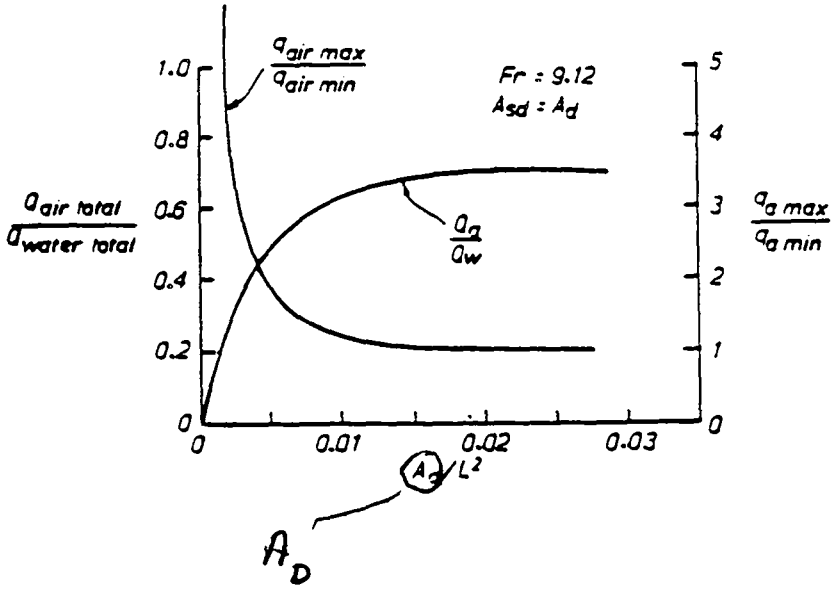

Fig. 4.22 An example of the effect of a change in the air duct area on the air demand and the air distribution [Rutschmann, Volkart and Wood, 1986]

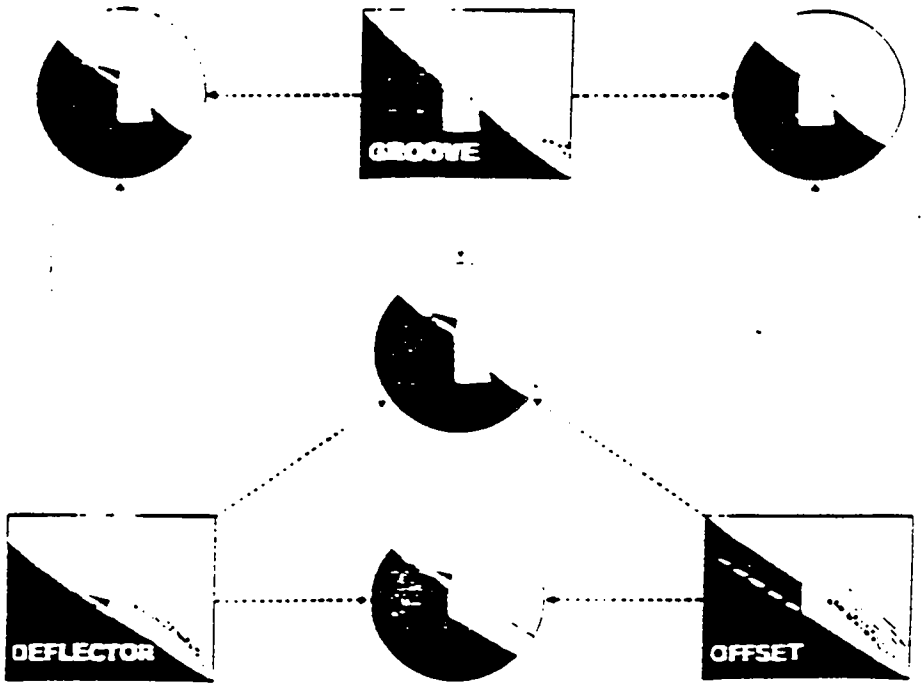

Fig. 4.23 The main aeration devices and their combinations. (Schematic longitudinal section)

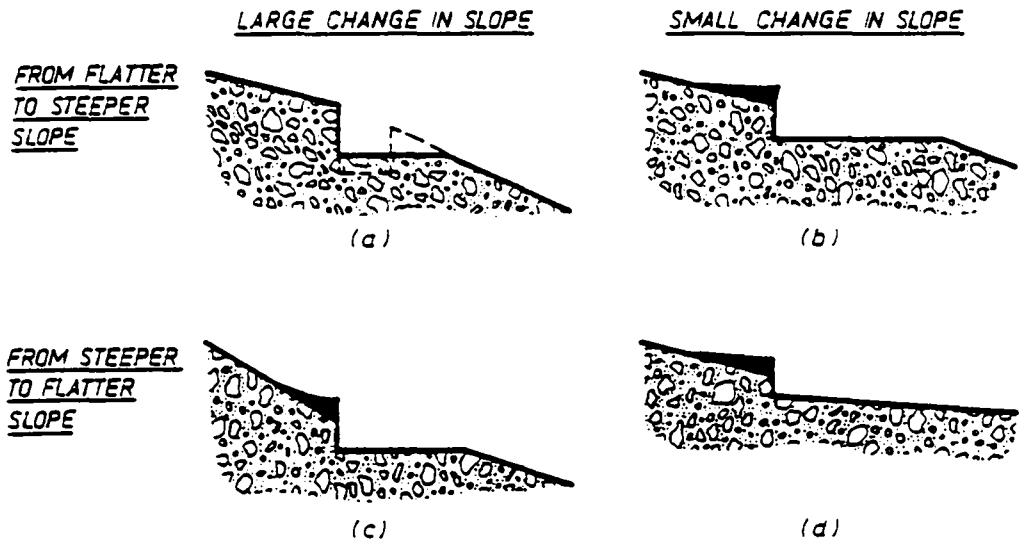

Fig. 4.24 Aerators at slope transitions

Type A

Type B

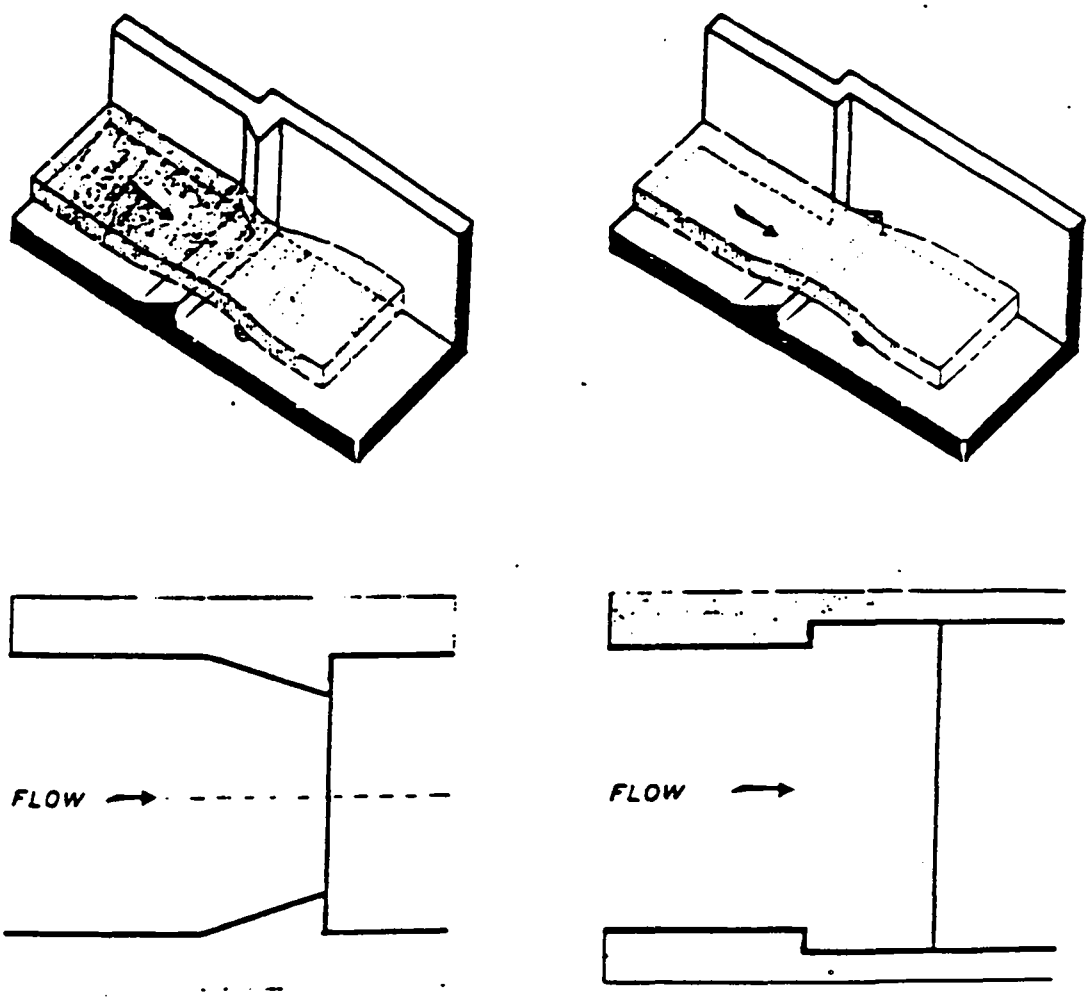

Fig.4.25 Examples of possible air supply systems

(a)

An air supply with lateral deflector e.g. Mantaro, Peru

(b)

An air supply with a lateral offset, e.g. Ait Chouarit, Maroc (bottom outlet)

Type C

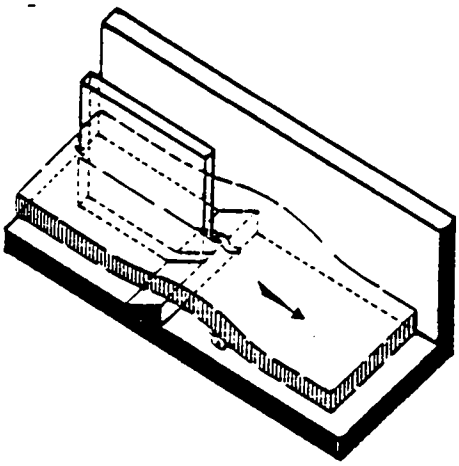

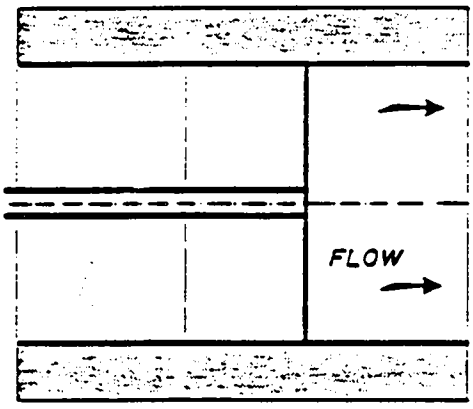

Figure 4.25(c)

Air supply behind pier,

e.g. Clyde Dam, New Zealand

Type D

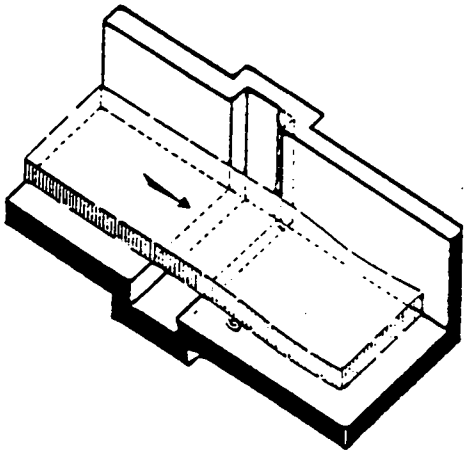

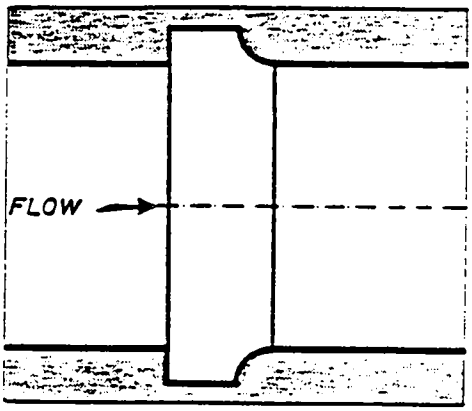

Figure 4.25(d)

Air supply by lateral grooves,

e.g. Calacuccia, France

Type E

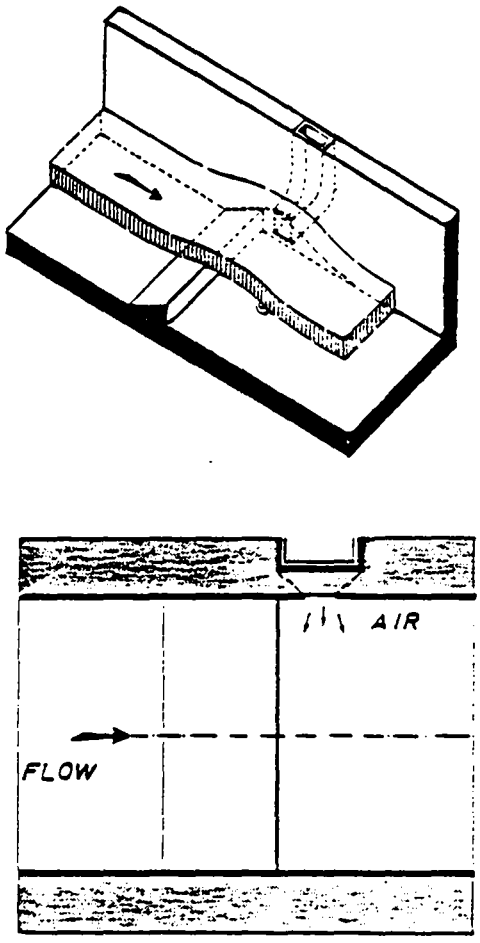

Figure 4.25(e)

Air supply by special air ducts below water jet, e.g. Foz do Areia, Brazil